

The Many Electron Ground State of the Adiabatic Holstein Model in Two and Three Dimensions

B. POORNACHANDRA SEKHAR, SANJEEV KUMAR AND PINAKI MAJUMDAR

*Harish-Chandra Research Institute,
Chhatnag Road, Jhusi, Allahabad 211 019, India*

(received ; accepted)

PACS. 71.38. – Polarons and electron-phonon interaction.

PACS. 71.45.L – Charge density wave systems.

PACS. 74.20. – Theory.

Abstract. –

We present the complete ground state phase diagram of the Holstein model in two and three dimension considering the phonon variables to be classical. We first establish the overall structure of the phase diagram by using exact diagonalisation based Monte Carlo (ED-MC) on small lattices and then use a new “travelling cluster” approximation (TCA) for annealing the phonon degrees of freedom on large lattices. The phases that emerge include a Fermi liquid (FL), with no lattice distortions, an insulating polaron liquid (PL) at strong coupling, and a charge ordered insulating (COI) phase around half-filling. The COI phase is separated from the Fermi liquid by a regime of phase coexistence whose width grows with increasing electron-phonon coupling. We provide results on the electronic density of states, the COI order parameter, and the spatial organisation of polaronic states, for arbitrary density and electron-phonon coupling. The results highlight the crucial role of spatial correlations in this strong coupling problem.

Introduction. – Electron-phonon (EP) interactions are ubiquitous in metals and dominate the finite temperature resistivity in most electron systems. While the perturbative, Fermi liquid, regime in EP systems is well understood [1], the electronic ground state is fundamentally reorganised when EP interactions are strong. The presence of a strong local interaction can generate a large lattice distortion, creating a potential well for the electron, and lead to a ‘self trapped’ polaronic state [2]. Strong electron-phonon coupling, sometimes in conjunction with other interactions, form a crucial component in the physics of several correlated systems, *e.g.* the manganites [3], the nickelates [4], and the traditional charge density wave systems [5].

The full ‘polaron problem’, considering the quantum dynamics of the phonons and strong EP coupling, is well understood for a single (or few) electrons [6, 7, 8, 9]. The non perturbative nature of the problem and the exponential growth in Hilbert space with electron number, N_{el} , has made the finite density problem difficult to access. Usually, the physical interest is in the “adiabatic” regime since typical phonon frequencies in most materials are much smaller than the electron hopping scale. Although adiabaticity by itself does not lead to a simpler problem,

the *adiabatic limit*, where phonon dynamics is ignored, leads to a relatively tractable situation. This limit, of electrons coupled to classical phonons, has been explored within dynamical mean field theory (DMFT) [10, 11, 12]. DMFT, however, loses out on spatial correlations or the possibility of accessing inhomogeneous phases, important at strong coupling. In this paper we use an approach that *explicitly retains spatial correlations* and set out the ground state of many electron systems, in two and three dimension, coupled to adiabatic phonons.

Let us define the Holstein model, whose adiabatic limit we explore:

$$H = -t \sum_{\langle ij \rangle} c_i^\dagger c_j - \mu \sum_i n_i - \lambda \sum_i n_i x_i + \frac{1}{2M} \sum_i p_i^2 + \frac{K}{2} \sum_i x_i^2 \quad (1)$$

The t are nearest neighbour hopping on a d dimensional lattice, μ is the chemical potential, and $n_i = c_i^\dagger c_i$ is the electron density operator for spinless fermions. The phonon coordinate is x_i , and p_i is the momentum conjugate to x_i , with $[x_i, p_j] = i\delta_{ij}$. M and K are respectively the ‘mass’ and stiffness of the phononic oscillators, and λ is the EP coupling. We set $t = 1$, as our reference scale, put $K = 1$ and also $\hbar = 1$. The adiabatic limit sets $M \rightarrow \infty$. For ‘quantum’ phonons, with $\omega_{ph} = \sqrt{K/M}$, the last three terms in H can be written as: $-\lambda_Q \sum_i n_i (b_i^\dagger + b_i) + \omega_{ph} \sum_i b_i^\dagger b_i$, using $x_i = (b_i + b_i^\dagger)/\sqrt{2M\omega_{ph}}$, and $\lambda_Q = \lambda\sqrt{\omega_{ph}/(2K)}$.

The parameter space of the model is defined by: (i) the ‘coupling parameter’ $\alpha = E_p/2dt$, with $E_p = \lambda^2/2K$, (ii) the ‘adiabaticity’ $\gamma = \omega_{ph}/t$, and (iii) electron density, n , in addition to dimensionality, d . The parameter α quantifies the competition between trapping and delocalisation, while γ measures the ‘slowness’ of the phonons compared to electron dynamics.

The ground state of this model is understood only in a few limiting cases: (i) At weak to moderate coupling, traditional Migdal-Eliashberg (ME) theory [13] can be used for the many electron problem for $\gamma \ll 1$, and describes a Fermi liquid (FL) metal (or a superconductor). (ii) At strong coupling, and for arbitrary γ , there is no controlled analytic theory even for a single electron coupled to the phonon system. There are, however, powerful numerical methods and the ‘single polaron’ ground state is essentially understood [6, 7, 8, 9]. Little is known of the many electron problem beyond ME theory. (iii) Controlled theory of strong coupling finite density systems has been possible only in the classical limit, $\gamma = 0$, in the limit $d \rightarrow \infty$. The original study by Millis *et al.* [10] highlighted the FL and polaronic insulator phases, within DMFT, and other DMFT studies have explored charge ordering [11, 12].

While contributing to the initial understanding, DMFT misses out on some crucial aspects of the physics. (i) The spatial correlation of lattice distortions, and the resulting correlations between polarons, when they form, is not accessible, and (ii) the possibility of phase coexistence and cluster formation is hard to access. We need to move beyond DMFT to recover these physical effects, and address current materials issues. The method we use, described next, can handle many electron systems strongly coupled to adiabatic phonons, at arbitrary disorder, explicitly in 1 – 3 dimension. This paper focuses on the ground state of ‘clean’ systems, subsequent papers discuss the finite temperature effects and the role of disorder [14].

Method. – At low temperature the adiabatic EP problem reduces to finding the phonon configuration that would minimise the total energy: $\mathcal{E}\{x\} = \langle -t \sum_{\langle ij \rangle} c_i^\dagger c_j - \mu \sum_i n_i - \lambda \sum_i n_i x_i \rangle_{\{x\}} + (K/2) \sum_i x_i^2$. At strong coupling the electronic energy (in angular brackets) in a phonon background, $\{x\}$, is not analytically known, since the problem is equivalent to that of electrons in an *arbitrary* strongly fluctuating landscape. The only unbiased way to solve the problem is to generate Monte Carlo samples of the phonon configurations and accept or reject them using the fermion energy obtained by exact diagonalisation [15]. Such exact diagonalisation based Monte Carlo (ED-MC) is feasible only for electronic Hilbert space

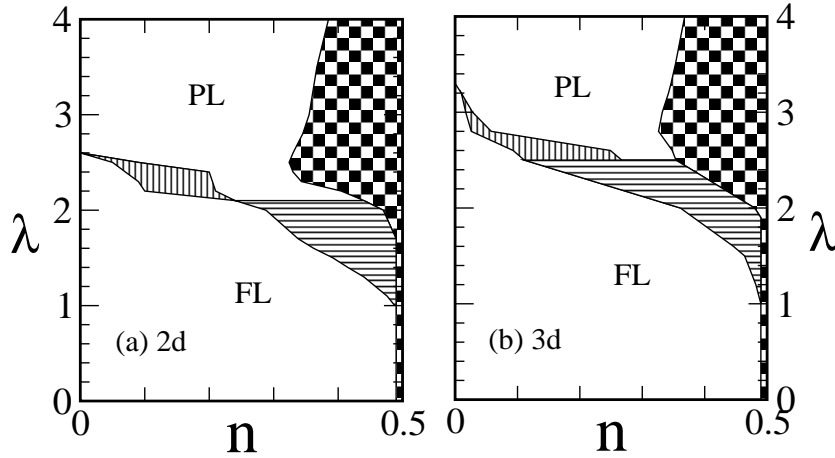


Fig. 1. – Phase diagrams at $T = 0$. FL indicates Fermi liquid (band metal), the chessboard pattern represents a charge ordered insulator with $\{\pi, \pi, \dots\}$ modulation, and PL is a positionally disordered insulating polaron liquid. Shading indicates regimes of phase separation. The phase diagrams are obtained through a combination of TCA and analytic estimates: (a) result on 2d, TCA with $L_c = 4$ and system size 24^2 , (b) result on 3d with $L_c = 4$ and system size 8^3 . The coexistence width at weak coupling is estimated as explained in the text.

dimension H_N upto ~ 100 since the computation time τ_N grows as H_N^4 . Although the finite size effects are quite strong, the small sizes do provide a feel for the phase diagram. Our ‘reference results’ in 2d and 3d are based on ED-MC on 8^2 and 4^3 systems.

To overcome the severe size limitation of ED-MC we have used a ‘travelling cluster’ approximation [16] (TCA) for estimating the energy change due to a phonon move. Thus, instead of estimating the energy change of the update $x_i \rightarrow x'_i$, at site \mathbf{R}_i , as $\Delta\mathcal{E} = \mathcal{E}\{x'\} - \mathcal{E}\{x\}$, by diagonalisation of the full Hamiltonian, we obtain an estimate from a ‘cluster’ Hamiltonian constructed by considering L_c^2 (or L_c^3) sites around the reference site \mathbf{R}_i . The energy of the system as a whole of course cannot be approximated by the energy, $\mathcal{E}_{cl}\{\mathbf{R}_i\}$, of the cluster, but the *change in the energy of the system* when a phonon update is made is accurately captured by the smaller subsystem. We have broadly benchmarked TCA against ED-MC in an earlier paper [16], and also provide several comparisons between the exact and TCA results in this paper. Our large size TCA results are obtained by using 4^2 clusters on 24^2 systems in two dimension, and 4^3 clusters on 8^3 in three dimension.

To allow effective annealing we study the system at low finite temperature, $T = 0.02$, with varying μ . At equilibrium, at a given μ , we calculate the following: (i) the electron density, $n(\mu)$, (ii) the structure factor $S(\mathbf{q}) = (1/N^2) \sum_{ij} \langle n_i \rangle \langle n_j \rangle e^{i\mathbf{q} \cdot (\mathbf{R}_i - \mathbf{R}_j)}$, including $S(\pi, \pi, \dots)$, the order parameter for commensurate charge ordering ($\langle n_i \rangle$ is the quantum average of n_i in a MC configuration and the outer angular brackets indicate average over configurations), (iii) the electronic density of states (DOS), $N(\omega)$, (iv) the distribution of lattice distortions, as well as MC snapshots of the electron density. Fig.1 sets out the ground state phase diagram in 2d and 3d, while the detailed indicators, like $n(\mu)$, $S(\pi, \pi, \dots)$, and $N(\omega)$, from which the phase diagram is constructed, are shown in Figs.2-3. To access the ‘weak coupling’ part of the phase diagram, $\lambda < 1.5$ say, we have used an analytic method described later.

Phases. – The two panels in Fig.1 show the asymptotic large L phase diagram obtained through a combination of TCA and analytic estimates. Our simulations reveal that there

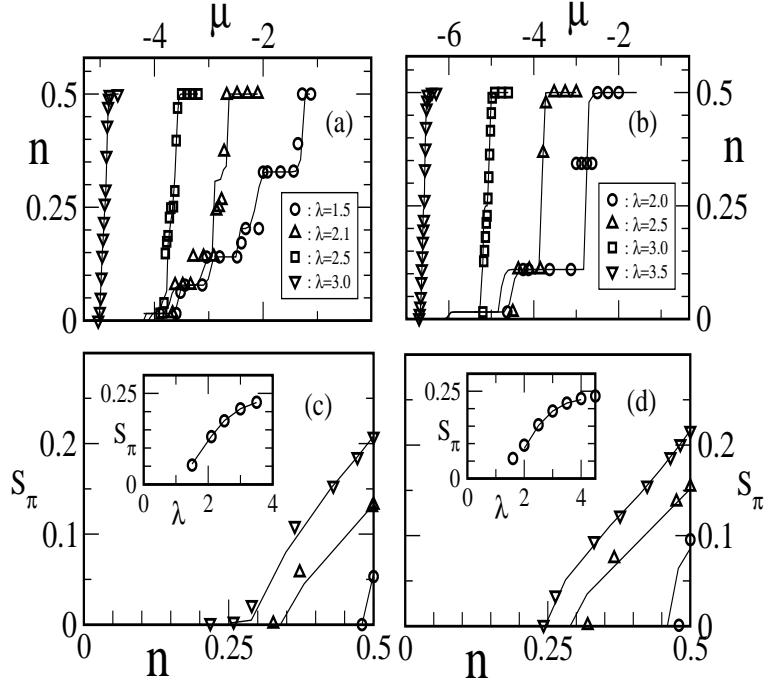


Fig. 2. – Panels (a) and (b) show the variation in carrier density with μ computed with ED-MC (symbols) and TCA (lines). Panel (a) is for 2d, with ED on 8^2 and TCA with 4^2 on 8^2 , while (b) is for 3d, with ED on 4^3 and TCA with 3^3 on 4^3 . Panels (c) and (d) show the COI ‘order parameter’ with varying electron density and coupling. Panel (c) is for 2d, panel (d) is for 3d. Symbols for ED, firm lines for TCA, same system size as in (a) – (b). The insets to the lower panels show the COI order parameter at $n = 0.5$. TCA on large sizes does not significantly change the $T \rightarrow 0$ order parameter. Panel (a) and (c) share a common legend, as do panel (b) and (d).

are primarily three phases in the adiabatic limit, for $T \rightarrow 0$, in both 2d and 3d. These are (i) the FL phase, *i.e.*, the tight binding electron system, without any lattice distortions, (ii) an insulating polaron liquid (PL) with no positional order and a gap in the DOS, and (iii) charge ordered insulating (COI) phases, with a gap in the DOS, and a peak at $\mathbf{q} = \{\pi, \pi, \dots\}$ in $S(\mathbf{q})$. The COI is either a simple ‘‘chessboard’’ phase at $n = 0.5$, or a phase with ‘‘defects’’ off $n = 0.5$ (and strong coupling). There is also the possibility of other charge ordered phases, apart from $\{\pi, \pi, \dots\}$, in the vicinity of $n = 1/4, 1/8, \dots$, at strong coupling, but their energy difference with respect to the PL phase is very small, making it difficult to access them in a low but finite T simulation. There are no ‘‘metallic’’ phases with lattice distortions, unlike suggested by DMFT [10]. We discuss the phase diagram in terms of the two broad regimes: (i) strong coupling polaronic phases, and (ii) weak coupling: the COI instability and phase separation.

(i) *Strong Coupling:* A naive balance of the ‘polaron binding energy’ $E_p = \lambda^2/2K$ (for a site localised electron), and the lower edge of the tight binding band, $-E_b = 2dt$, suggests that polaron formation would occur at $\lambda_c \approx \sqrt{4Kdt}$, implying $\lambda_c^{2d} \sim 2.82$ and $\lambda_c^{3d} \sim 3.46$. More accurate earlier estimates [7], and our simulations, indicate $\lambda_c^{2d} \sim 2.6$ and $\lambda_c^{3d} \sim 3.3$. The lowering arises because the polaron is not quite site localised, and taking into account the kinetic energy $\sim dt^2/E_p$, the polaronic state becomes favourable slightly before the naive threshold. The polaron states which emerge for $\lambda \geq \lambda_c$ are compact, although not site localised, with wavefunctions decaying over a couple of lattice spacings. Due to the strong

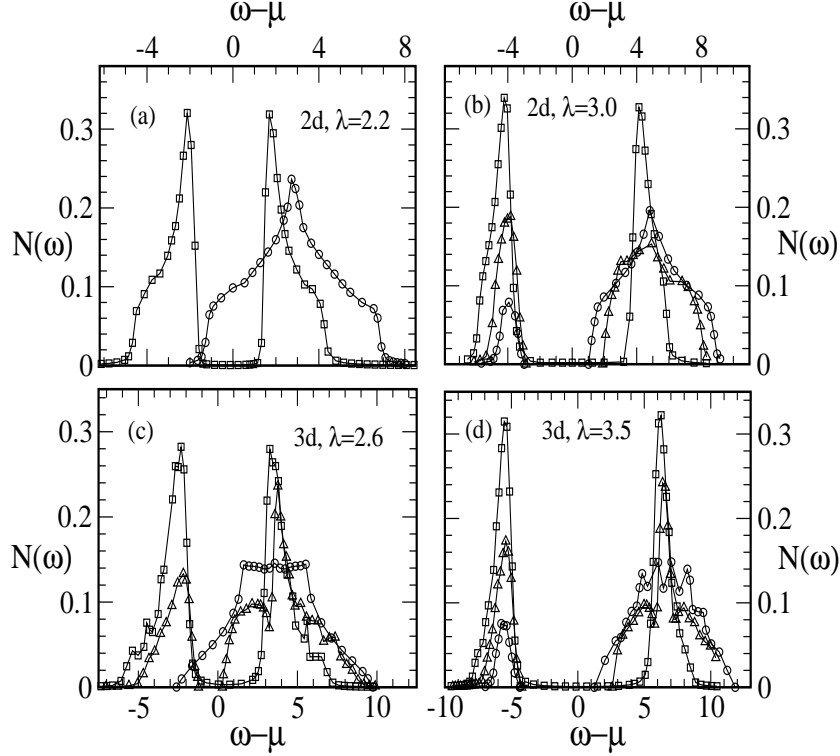


Fig. 3. – Density of states computed with TCA on 24×24 in 2d, and $8 \times 8 \times 8$ in 3d. Symbols: circles for $n = 0.1$, triangles for $n = 0.3$, and squares for $n = 0.5$. (a) 2d, $\lambda = 2.2$, (b) 2d, $\lambda = 3.0$, (c) 3d, $\lambda = 2.6$, (d) 3d, $\lambda = 3.5$.

localisation, and the associated short range lattice distortion field, the *finite density* system is a random array of trapped electrons (the PL phase), keeping maximum mutual separation in order to maximise kinetic energy gain by virtual hopping. The polarons are effectively like “hardcore” classical particles, interacting via short range weak repulsion $\sim \mathcal{O}(t^2/E_p)$ for nearest neighbours. The repulsion favours a “chessboard” CO phase at $n = 0.5$.

The off half-filling phase maintains the positional correlations of the $n = 0.5$ phase, but has vacancies (or defects), see *e.g.* Fig.4. The polarons tend to avoid nearest neighbour locations, preferring to be along the diagonal (where the ‘repulsion’ is weaker). As long as the system is sufficiently dense, these positional correlations ‘percolate’ sustaining long range order, with a clear peak in $S(\pi, \pi, \dots)$. Our results suggest that the strong coupling off half-filling COI phase survives down to a density ≈ 0.35 in the coupling regime shown (Fig.1). The order parameter for the COI phases is shown in Fig.2.(c) – (d), and the DOS in Fig.3. The order parameter computed with TCA on small sizes, see Fig.2 caption, accurately matches ED-MC results. TCA results on large sizes for $S(\pi, \pi, \dots)$ (not shown) are not significantly different.

The critical coupling for the FL to PL transition is *density dependent*, decreasing significantly, Fig.1 (c) – (d), from the single polaron threshold as n is increased. By the time $n \sim 0.3 - 0.4$, λ_c is reduced to $\approx 75\%$ of the ‘single polaron’ value, in both 2d and 3d, *i.e.* the critical E_p is almost halved. Qualitatively, electrons which are already localised affect an added particle via their strongly inhomogeneous distortion field, $\{x\}$, which interplays with EP coupling leading self consistently to the decreasing $\lambda_c(n)$. Trapping at finite n involves a

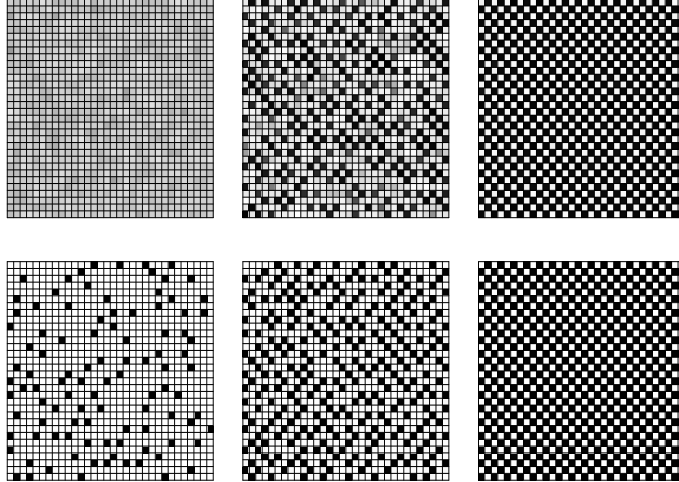


Fig. 4. – Monte Carlo snapshots of the electron density n_r with varying n and λ in 2d. Top panels $\lambda = 2.2$, bottom panels $\lambda = 3.0$. Density $n = 0.10, 0.30, 0.50$, left to right. Top left panel is FL. Both panels to the extreme right are ‘perfect’ COI, while the other three panels are PL.

combination of (self generated) “disorder” and polaronic tendency [17], akin to the interplay of Anderson localisation and single polaron formation.

All the phases, COI or PL, which occur for $\lambda \geq \lambda_c(n)$ have a clear spectral gap, and are distinguished mainly by $S(\mathbf{q})$. The “edges” of the DOS in the PL phase, see Fig.3 (b) – (d), are similar to that in the COI phases, resulting from short range positional correlations.

(ii) *Weak Coupling:* At weak coupling there is an instability in a bipartite tight binding lattice, at $n = 0.5$, due to Fermi surface nesting. The density response function $\chi(\mathbf{q}, \omega = 0)$ diverges for $\mathbf{q} \rightarrow \{\pi, \pi, \dots\}$. For $\lambda \rightarrow 0$, where the analysis in terms of the non interacting susceptibility is valid, this leads to a charge order instability, with ordering temperature $T_{CO} \sim te^{-t/E_p}$. With increasing λ the CO phase continues to be the ground state, but as the charge modulation increases, and the band splitting grows, the FL to COI transition at $T = 0$ becomes *first order*, since the electron density in the modulated x_i background is significantly different from that in the homogeneous background. The $n - \mu$ data in Fig.2. (a) – (b) highlight the discontinuity in n near half-filling. It is difficult to access the instability and the coexistence width at weak coupling in a small system since $\chi(\mathbf{q}, \omega = 0)$ has strong size dependence. Direct simulation can locate the CO phase only down to $\lambda \sim 1.5$. At lower λ we variationally computed the COI order parameter at $n = 0.5$ on large lattices, and also the $\mu_c(\lambda)$ at which the FL to COI transition occurs. It suggests that the FL to COI transition becomes (noticeably) first order for $\lambda \geq 1.0$, in both 2d and 3d. The weak coupling COI phase at $n = 0.5$ connects continuously to the strong coupling “polaron ordered” phase [11, 12].

Discussion. – Despite accurate handling of strong coupling and spatial correlations, a few physical effects in the adiabatic limit are still difficult to capture within a numerical simulation. Other effects, of possible relevance to real materials, require us to go beyond the adiabatic limit itself. This section briefly discusses these issues.

(i) As we have discussed, even in the adiabatic limit, there are possibly additional commensurate CO phases at $n = 1/4, 1/8$ etc, which could show up at very low temperature. There

could also be *incommensurate* CO phases at weak coupling, these are hard to access on small systems, given the strong finite size effects in $\chi(\mathbf{q}, \omega = 0)$.

(ii) In real materials ω_{ph} would be finite, and quantum fluctuations would modify some of our conclusions: (a) The simple ‘band metal’ (FL) obtained at $\omega_{ph} = 0$ would become a correlated Fermi liquid, with effective mass renormalisation, band narrowing, *etc*, if $\omega_{ph} \neq 0$, and could even become superconducting (SC). At weak coupling this would be a BCS instability setting in at $T_{SC} \sim \omega_{ph} e^{-1/N(\epsilon_F)E_p}$, away from $n = 0.5$ [18]. (b) Quantum fluctuations would restore translation invariance in the PL phase [19] so that below a coherence scale, $T_{coh} \sim \omega_{ph}$, the resistivity falls quickly to zero, instead of diverging as the gapped DOS here would suggest. (c) The COI phase would survive for $n \sim 0.5$ but may have to compete with SC sufficiently away from $n = 0.5$. There are some results on this competition within DMFT at weak coupling [18] as well as strong coupling [20]. As long as $\omega_{ph}/t \ll 1$, our “ground state” phase diagram would be qualitatively useful for $T > T_{coh}$ (or T_{SC}) in the problem.

In summary, we have used a new real space method that naturally incorporates the spatial correlations vital at metallic densities, to clarify the phase diagram of the adiabatic Holstein model. This approach allows unconstrained optimisation, not restricted to any specific kind of order, and readily reveals the regimes of phase coexistence. It also extends naturally to incorporate the effects of disorder and thermal fluctuations [14]. Another possibility, we will separately report, is to include spin degrees of freedom, via double exchange, to model the phenomena in manganite physics.

Acknowledgement We acknowledge use of the Beowulf cluster at H.R.I.

REFERENCES

- [1] J. M. Ziman, *Electrons and Phonons*, Oxford University Press, New York (1960), see also G. D. Mahan, Chapters 4 and 6 of *Quantum Many Particle Physics*, Plenum Press, New York (1990).
- [2] For a general reference see, *e.g.*, A. S. Alexandrov and N. F. Mott, *Polarons and Bipolarons*, World Scientific, Singapore (1995).
- [3] *Colossal Magnetoresistive Oxides*, edited by Y. Tokura, Gordon and Breach, Amsterdam (2000).
- [4] C. H. Chen, S. W. Cheong and A. S. Cooper, Phys. Rev. Lett. **71**, 2461 (1993), J. Zaanen and P. B. Littlewood, Phys. Rev. **B 50**, 7222 (1994).
- [5] G. Gruner, *Density Waves in Solids*, Addison-Wesley, New York (1994).
- [6] P. E. Kornilovitch, Phys. Rev. Lett. **81**, 5382 (1998).
- [7] A. H. Romero, D. W. Brown and K. Lindenberg, Phys. Rev. **B 60**, 14080 (1999).
- [8] J. Bonca, S. A. Trugman, and I. Batistic, Phys. Rev. **B 60**, 1633 (1999).
- [9] A. S. Alexandrov, V. V. Kabanov, and D. K. Ray, Phys. Rev. **B 49**, 9915 (1994), V. V. Kabanov and O. Yu. Mashtakov, Phys. Rev. **B 47**, 6060 (1993).
- [10] A. J. Millis, R. Mueller, and B. I. Shraiman, Phys. Rev. **B 54**, 5389 (1996).
- [11] S. Ciuchi and F. de Pasquale, Phys. Rev. **B 59**, 5431 (1999).
- [12] S. Blawid and A. J. Millis, Phys. Rev. **B 62**, 2424 (2000).
- [13] A.B. Migdal, Sov. Phys. JETP **7**, 996 (1958), G.M. Eliashberg, Sov. Phys. JETP **11**, 696 (1960).
- [14] Sanjeev Kumar and Pinaki Majumdar, cond-mat 0406084.
- [15] see, *e.g.*, J. A. Verges, V. Martn-Mayor, and L. Brey, Phys. Rev. Lett. **88**, 136401 (2002).
- [16] Sanjeev Kumar and Pinaki Majumdar, cond-mat 0406082.
- [17] See, *e.g.*, D. Emin and M.-N. Bussac, Phys. Rev. **B 49**, 14290 (1994) for the interplay of *extrinsic* disorder and EP coupling.
- [18] S. Ciuchi, F de Pasquale, C. Masciovecchio and D. Feinberg, Europhys. Lett. **24**, 575 (1993).
- [19] S. Fratini and S. Ciuchi, Phys. Rev. Lett. **91**, 256403 (2003).
- [20] J. K. Freericks, M. Jarrell and D. J. Scalapino, Phys. Rev. **B 48**, 6302 (1993).